Min Sub Sim

Sulfur Isotope Fractionation during the Thiosulfate Disproportionation Reaction

1. Introduction

Although the sulfur isotope fractionation by sulfate-reducing bacteria has been interpreted as a common mechanism for the ^{34}S depletion of sedimentary sulfide, the activity of sulfate reducing bacteria causing an isotope fractionation up to 46 per mil (Chambers et al., 1975) cannot account for the large depletion in marine sediments which is commonly between 35 and 60 per mil (Canfield and Teske, 1996). Hence, additional isotope fractionation process during the marine sulfur cycle needs to explain such a large depletion. The disproportionation process of various sulfur species of the oxidative sulfur cycle, which follows the sulfate reduction, is thought to contribute the ^{34}S depletion of sedimentary sulfide because it generates sulfides more depleted in ^{34}S than the original sulfide produced by sulfate reducing bacteria (Jorgensen, 1990; Canfield and Thamdrup, 1994). However, the detail isotope fractionation mechanism during the disproportionation reaction is not clarified yet.

There are various sulfur species participating in the disproportionation reaction such as elemental sulfur (S^0), sulfite (SO_3^{2-}), and thiosulfate ($S_2O_3^{2-}$). Among them, this study mainly deals with the disproportionation reaction of thiosulfate. Thiosulfate has two sulfur atoms of which the inner one is the oxidized sulfonate sulfur, while the outer one is the reduced sulfane sulfur. During the disproportionation reaction, sulfonate sulfur is mainly converted to sulfate, whereas about 90% of sulfane sulfur is converted to sulfide (Jorgensen, 1990). Such a process presents two possibilities to generate ^{34}S-depleted sulfides and ^{34}S-enriched sulfate through the bacterial disproportion reaction. One is that sulfur disproportionation bacteria preferentially cleave the bond between light sulfane sulfur and heavy sulfonate sulfur compared to the opposite case (kinetic control). The other is that regardless of the disproportionation reaction, sulfonate sulfur is initially enriched in ^{34}S relative to sulfane sulfur through the equilibrium process or biologically-mediated kinetic process. In this study, therefore, the isotope fractionation process during the bacterial thiosulfate disproportionation reaction is reviewed and examined based on quantum chemical calculations and previous experimental data.

2. Previous studies: experimental results

Review of bacterial thiosulfate disproportionation process (Habicht et al., 1998)

The bacterial sulfur disproportionation reaction consists of two steps: division of thiosulfate into sulfide and sulfite, and oxidation of sulfite to sulfate. Figure 1 shows the sulfur isotope fractionation among thiosulfate, sulfide, and sulfate during the bacterial thiosulfate

disproportionation process. As can be seen, there is no isotope fractionation associated with the formation of sulfate from the sulfonate sulfur, while the fractionation of about 4 per mil is observed through the formation of sulfide from sulfane sulfur. It may suggest that the bond associated with light sulfane sulfur is preferentially cleaved by bacteria. In my view, however, it is not certain whether this small fractionation is due to the kinetically-controlled bacterial process, or rapid equilibrium isotope exchange reaction between sulfide and sulfane sulfur which will be described in the following section. In addition, figure 1 shows another isotopic development between sulfur species. The reduced compounds including sulfide and sulfane sulfur became depleted in ^{34}S over time, whereas the oxidized compounds, sulfate and sulfonate sulfur, show the opposite trend. During the disproportionation reaction, there would be no chemical transformation between reduced and oxidized sulfur; therefore, an isotopic exchange reaction between reduced and oxidized sulfur could only explain this result. In particular, the similar depleting trend of sulfide and sulfane sulfur as well as the similar enriching trend of sulfate and sulfonate sulfur indicates that the isotope exchange would mainly occur between sulfonate and sulfane sulfur. Because abiogenic isotope exchange between sulfane and sulfonate sulfur was measured at temperature only above 100^{o}C (Uyama et al., 1985), above evidence strongly suggests that at low temperature the isotope exchange between sulfonate and sulfane sulfur should be mediated by bacterial activity. However, it is still not clear how bacteria activity facilitates the isotope exchange reaction between sulfane and sulfonate sulfur.

Review of nonbacterial sulfur isotope exchange reactions (Uyama et al., 1985; Chu et al., 2004)

Experimental data about the inorganic sulfur isotope exchange reaction was presented by Uyama et al. (1985), and further discussed by Chu et al. (2004). Figure 2 displays the variation with time of the isotope composition of thiosulfate, sulfate, and sulfide. It clearly shows that the isotope exchange between sulfane and sulfonate sulfur is only catalyzed by the isotope exchange reaction between thiosulfate and sulfide. Although in the sample containing only thiosulfate at the beginning the isotope exchange occurred after 200 hours (Figure 2A), it is probably due to the decomposition of thiosulfate, resulting in the proper concentration of sulfide. On the other hand, sulfate hindered the isotope exchange between sulfane and sulfonate sulfur (Figure 2C). Figure 3 presents the variation with time of the sulfur isotope composition of thiosulfate and sulfide at various temperatures. It indicates that the isotope exchange reaction among sulfide, sulfonate, and sulfane sulfurs proceed at temperature over 100^{o}C, and the exchange rate increases with increasing temperature. At 50^{o}C, the isotope exchange only between sulfide and sulfane sulfur occurred. According to these results, presence of sulfide and the temperature higher than 100^{o}C are the prerequisites for the non-bacterial isotope exchange reaction between sulfonate and sulfane sulfur. However, the detailed isotope exchange reaction is actually more complicated because the

isotope exchange between thiosulfate and sulfide is achieved through the intermediate step, the formation of polysulfide. At high temperature, the formation rate of polysulfides is so fast that the isotope equilibrium can be attained through the isotope exchange via polysulfides. At low temperature and the given composition of sulfur species, however, the formation rate of polysulfides may be slow, and thus the isotopic equilibrium cannot be obtained within the experimental period.

3. Method

Reduced partition function ratio

The differences in the energy levels of the isotope are the fundamental cause of equilibrium isotope fractionation, and these energy differences can be calculated based on the vibration frequencies of molecules containing isotopes. Hence, if the vibration frequencies of isotopomers are known, one can theoretically predict the isotope fractionation factor using the reduced partition function ratio (Bigeleisen and Mayer, 1947; Urey, 1947). Since this theory was first introduced, it has been used to calculate the equilibrium fractionation factors for various isotope systems (Richet et al., 1977; Yanase and Oi, 2002; Schauble et al., 2004; Anbar et al., 2005; Zeebe, 2005; Seo et al., 2007). In this paper, therefore, the theory is briefly reviewed rather than explicated in detail.

Considering the isotope exchange reaction in which only one sulfur atom is exchanged, the reaction between two sulfur species can be written as follows:

$$A^{32}S + B^{34}S = A^{34}S + B^{32}S$$

where A and B are polyatomic groups. In this reaction, the equilibrium constant of the equation (K_{eq}) is identical to the fractionation factor ($\alpha_{AS\text{-}BS}$).

$$\alpha_{AS\text{-}BS} = K_{eq} = (A^{34}S) \times (B^{32}S) / (A^{32}S) \times (B^{34}S) = \beta_{34\text{-}32}(AS) / \beta_{34\text{-}32}(BS)$$

Then, in order to predict the fractionation factor, the reduced partition function ratio of each molecule containing sulfur isotope should be calculated. This ratio is defined by:

$$\beta_{34\text{-}32} = \prod_{i=1}^{3N-6} \frac{^{34}U_i}{^{32}U_i} \cdot \frac{^{34}Q_{vib}}{^{32}Q_{vib}} = \prod_{i=1}^{3N-6} \frac{^{34}U_i}{^{32}U_i} \cdot \frac{e^{-^{34}U_i/2}}{e^{-^{32}U_i/2}} \cdot \frac{1-e^{-^{32}U_i}}{1-e^{-^{34}U_i}}$$

where

$$Ui = h\nu_i / kT$$

Here, h and k are the Plank and Boltzman constants, respectively. N is the number of each species; therefore, 3N-6 is the number of normal mode vibrations, T is the temperature (K), ν_i is the vibration frequency of each isotopomer, and Q_{vib} is the vibration partition function. Finally, fractionation factor and the isotope compositions expressed in terms of δ values can be correlated by:

$$1000 \times \ln(\alpha_{AS\text{-}BS}) \approx \delta^{34}S_{AS} - \delta^{34}S_{BS}$$

For the convenience, the reduced partition function ratios are expressed as the form of $1000 \times \ln(\beta_{34\text{-}32})$ following previous studies (Schauble et al., 2004; Anbar et al., 2005; Seo et al., 2007).

Computational methods

Geometry optimization and vibrational frequency calculations were done using quantum chemical program Gaussian03 (Frisch et al., 2003). Calculated molecules include HS^-, H_2S, SO_4^{2-}, and $S_2O_3^{2-}$. Hartree-Fock (HF) calculations with 6-21G* basis set without symmetry constraints of molecules were used for all geometry optimization. It yields optimized geometry without negative frequencies. The vibrational frequencies were also calculated using HF method with 6-31G* basis set. For the geometry optimization and calculation of the vibration frequencies, the solution effects were included using the polarizable continuum model (PCM) (Miertus et al., 1981; Miertus and Tomasi, 1982) because thiosulfate disproportionation in the aqueous phase is responsible for the ^{34}S depletion of sedimentary sulfide. Predicted vibration frequencies were then used to obtain $\beta_{34\text{-}32}$ following above equations.

4. Results

The vibration frequencies of optimized molecules of HS^-, H_2S, SO_4^{2-}, and $S_2O_3^{2-}$ and substituted isotopomer were calculated with the HF method. Previous studies shows that HF method tends to overestimate the vibrational frequency. Therefore, all calculated frequencies were calibrated by the scaling factor 0.8928, which was calculated from the comparison between the experimentally observed vibration frequencies (Shimanouchi, 1972) and the theoretical vibration frequencies of H_2S. Using this scaling factor, calibrated frequencies of SO_4^{2-} are fairly in agreement with the previous reported data for SO_4^{2-} (Urey and Bradley, 1931). Hence, all calculated frequencies were calibrated by this scaling factor. In table 1, the calibrated vibration frequencies and frequency shifts are listed.

Table 2 and figure 4 show the calculated reduced partition function ratios, $10^3 \times \ln(\beta_{34\text{-}32})$, of sulfur species with varying temperature from 50 K to 1200 K, including thetemperature range of Uyama et al. (1985)'s experiment. As can be seen, sulfate shows the largest reduced partition function ratios and HS^- has the smallest reduced partition function ratios. They show that the oxidation state of S is a major factor controlling inorganic isotope fractionation.

Figure 5 presents the calculated $10^3 \times \ln\alpha$ values of sulfonate S-H_2S, sulfane S-H_2S, HS^--H_2S, and SO_4^{2-}-H_2S along with the experimental data and calculated curves. The temperature-dependent trends in this study are consistent with the experimental data. Over 100°C at which the isotopic equilibrium among sulfur species had been observed in the experiments, calculated

10^3 x lnα values reasonably agree with the experimental data. In particular, that of SO_4^{2-}-H_2S is almost identical to the experimental data. In the case of other sulfur species, deviations from the experimental data are less than 5‰.

5. Discussions

A direct comparison of the calculated results to the experimental or natural data is not easy because not only a theoretical calculation cannot consider all the factors involved in the natural process but also our knowledge about the transition state is insufficient. In spite of such uncertainty, however, the comparison between the theoretical and experimental data is still helpful to understand the S isotope fractionation. In this study, the temperature-dependent trends of 10^3 x lnα values between sulfur species are consistent with the experimental data, whereas the absolute values slightly deviate from the corresponding experimental data. This result increases confidence in the experimental determination of the temperature-dependent isotope fractionation between sulfur species. Also, such a little difference suggests the possibility that the discrepancy between them can be calibrated by using some scaling factors. If calibrated, it would be very helpful to understand the isotope fractionation at low temperature at which the equilibrium isotope composition is hardly attained through the experiment.

Because many bacteria cannot live at such high temperatures, understanding the isotope exchange reaction at low temperature is crucial to explain the isotope fractionation during the bacterial thiosulfate disproportionation process. It is still not clear how bacteria activity facilitates the isotope exchange reaction between sulfane and sulfonate sulfur. One possibility is that bacterial activities such as selective uptake or export of the specific sulfur compounds would shift the chemical equilibrium among sulfur species within the cell, resulting in the rapid formation of intermediaries via which the isotope exchange between sulfane and sulfonate sulfur can occur. It is reasonable because the reaction rate is dependent on both temperature and the concentration of reactant and product. In that case, the role of bacterial activity can be considered to promote an equilibrium process rather than kinetically control the isotope exchange reaction. Consequently, the experimental or natural data can be correlated to the calculated isotope fractionation. However, it is also possible that some bacterial activity would be actively involved in the isotope exchange reaction. Then, the isotope fractionation is not an equilibrium process, but is kinetically controlled, probably resulting in the isotope composition deviating from the isotopic equilibrium.

Since the neutral pH is favored by most thiosulfate disproportionation bacteria (Finster et al., 1998; Habicht et al., 1998; Jackson and McInerney, 2000), pH may affect the isotope composition of sedimentary sulfide. Comparing the calculated results using H_2S and HS^-, the influence of pH on the isotope fractionation between sulfur species can be indirectly inferred. As

shown in the figures 4 and 5, at neutral pH where HS^- is dominant, the isotope composition of sulfide may become more ^{34}S-depleted than that at low pH. However, the experimental or natural data are necessary to validate the theoretical results.

According to the Uyama et al. (1985)'s experiment, sulfate hinders the isotope exchange between sulfonate and sulfaine sulfur. It can be explained by the chemical equilibrium among sulfur species via the reaction:

$$S_2O_3^{2-} + H_2O = SO_4^{2-} + H_2S$$

In this reaction, abundant sulfate prevents the decomposition of thiosulfate, and thus the formation rate of polysulfides cannot reach the level fast enough to mediate the significant isotope exchange between sulfonate and sulfane sulfur. However, excluding the extreme case that the whole sulfide produced by sulfur disproportionation bacteria will be removed by oxidation or precipitation of sulfide minerals, sulfide is always available where the thiosulfate disproportionation bacteria are present. Hence, the influence of sulfate on the isotope exchange reaction during the bacterial sulfur disproportionation can be ignored.

Conclusively, reviewing previous studies and comparing experimental data with calculated results provide confidence in our understanding of the isotope fractionation during the bacterial thiosulfate disproportionation process. Also, it presents further steps to proceed in order to understand this complicated process more clearly. First, the computational calculation of possible intermediaries during the isotope exchange reaction using more accurate basis set will definitely improve our understanding of the isotope fractionation during the bacterial disproportionation process. In addition, to answer the question how bacteria mediate the isotope exchange reaction even at low temperature, physiological study about the thiosulfate metabolism should be conducted.

References

Anbar, A. D., Jarzecki, A. A., Spiro, T. G., 2005. Theoretical investigation of iron isotope fractionation between $Fe(H_2O)_6^{3+}$ and $Fe(H_2O)_6^{2+}$: Implications for iron stable isotope geochemistry. Geochimica et Cosmochimica Acta 69, 825-837.

Bigeleisen, J., and Mayer, M.G., 1947. Calculation of equilibrium constants for isotopic exchange reactions. Journal of Chemical Physics 15, 261–267.

Canfield D. E. and Teske A., 1996. Late Proterozoic rise in atmospheric oxygen concentration inferred from phylogenetic and sulphur-isotope studies. Nature 382, 127–132.

Canfield D. E. and Thamdrup B., 1994. The production of ^{34}S-depleted sulfide during bacterial disproportiontion of elemental sulfur. Science 266, 1973–1975.

Chambers, L. A., Trudinger, P. A., Smith, J. W., and Burns, M. S., 1975. Fractionation of sulfur isotopes by continuous cultures of *Desulfovibrio desulfuricans*. Canadian Journal of Mucrobiology 21, 1602-1607.

Chu, X., Ohmoto, H., and Cole, D. R., 2004. Kinetics of sulfur isotope exchange between aqueous sulfide and thiosulfate involving intra- and intermolecular reactions at hydrothermal conditions. Chemical Geology 211, 217-235.

Finster, K., Liesack, W., and Thamdrup, B., 1998. Elemental sulfur and thiosulfate disoproportionation by *Desulfocapsa sulfoexigenes* sp. nov., a new anaerobic bacterium isolated from marine surface sediment. Applied and Environmental Microbiology 64, 119-125.

Frisch, M. J., Trucks, G. W., Schlegel, H. B., Scuseria, G. E., Robb, M. A., Cheeseman, J. R., Montgomery, J. A., et al., 2003. Gaussian03. Gaussian Inc.

Fry, B., Gest, H., Hayes, J. M., 1986. Sulfur isotope effects associated with protonation of HS- and volatilization of H2S. Chemical Geology: Isotope Geoscience section 58, 253-258.

Habicht, K. S., Canfield, D. E., and Rethmeier, J., 1998. Sulfur isotope fractionation during bacterial reduction and disproportionation of thiosulfate and sulfite. Geochimica et Cosmochimica Acta 62, 2285-2595.

Jackson, B., and McInerney, M., 2000. Thiosulfate disproportionation by *Desulfotomachulum thermobenzoicum*. Applied and Environmental Microbiology 66, 3650-3653.

Jørgensen B. B., 1990. A thiosulfate shunt in the sulfur cycle of marine sediments. Science 249, 152–154.

Miertus, S., Scrocco, E., Tomasi, J., 1981. Electrostatic interaction of a solute with a continuum. A direct utilization of AB initio molecular potentials for the prevision of solvent effect. Chemical Physics 55, 117–129.

Miertus, S., Tomasi, J., 1982. Approximate evaluation of the electrostatic free energy and internal energy changes in solution processes. Chemical physics 65, 239–245.

Ohmoto, H. and Rye, R. O., 1979. Isotope of sulfur and carbon, in Barnes, H. L. Ed., Geochemestry of Hydrothermal deposits, John Wiley & Sons, p. 509-567.

Ohmoto, H. and Lasagaa, A.C., 1982. Kinetics of reactions between aqueous sulfates and sulfides in hydrothermal systems. Geochimica et Cosmocimica Acta 46, 1727-1745.

Richet, P., Bottinga, Y., Javoy, M., 1977. A review of hydrogen, carbon, nitrogen, oxygen, sulphur, and chlorine stable isotope fractionation among gaseous molecules. Annual Review of Earth and Planetary Sciences 5, 65-100.

Schauble, E., Rossman, G., Taylor, H. P., 2004. Theoretical estimates of equilibrium chromium-isotope fractionations. Chemical Geology 205, 99-114.

Seo, J. H., Lee, S. K., Lee, I., 2007. Quantum chemical calculations of equilibrium copper (I) isotope fractionations in ore-forming fluids. Chemical Geology 243, 225-237.

Shimanouchi, 1972. Tables of Molecular vibration frequencies consolidated volume I, National Bureau of Standards, 1-160.

Urey C. and Bradley C. A., 1931. The vibrations of pentatonic tetrahedral molecules. Physical review 38, 1969-1978.

Urey, H. C., 1947. The thermodynamic properties of isotopic substances. Jouranl of Chemical Society, 562-581.

Uyama F., Chiba H., Kusakabe M., and Sakai H., 1985. Sulfur isotope exchange reactions in the aqueous system: thiosulfate-sulfide-sulfate at hydrothermal temperature. Geochem. J. 19, 301–315.

Yanase, S., Oi, T., 2002. Molecular orbital estimation of reduced partition function ratio of lithum ions in ion exchanger phase of aqueous ion exchange systems. Nukleonika 47, 75-79.

Zeebe, R. E., 2005. Stable boron isotope fractionation between dissolved $B(OH)_3$ and $B(OH)_4^-$. Geochimica et Cosmochimica Acta 69, 2753-2766

cm^{-1}	HS^-			H_2S				SO_4^{2-}			
	$^{32}\nu$	$^{34}\nu$	$1000(1-^{34}\nu/^{32}\nu)$	Shimanouchi (1972)	$^{32}\nu$	$^{34}\nu$	$1000(1-^{34}\nu/^{32}\nu)$	Urey and Bradley (1931)	$^{32}\nu$	$^{34}\nu$	$1000(1-^{34}\nu/^{32}\nu)$
ν_1	2721.44	2718.93	0.92	1183	1338.58	1337.30	0.96	451	472.31	472.31	0.00
ν_2				2615	2858.93	2856.65	0.80	451	472.90	472.90	0.00
ν_3				2626	2871.10	2868.27	0.99	611	651.98	647.58	6.75
ν_4								611	652.21	647.83	6.72
ν_5								611	652.47	648.08	6.73
ν_6								983	1064.41	1064.41	0.00
ν_7								1105	1214.17	1198.19	13.16
ν_8								1105	1214.40	1198.41	13.17
ν_9								1105	1214.64	1198.66	13.16

cm^{-1}	Sulfane (SSO_3^{2-})			Sulfonate (SSO_3^{2-})		
	$^{32}\nu$	$^{34}\nu$	$1000(1-^{34}\nu/^{32}\nu)$	$^{32}\nu$	$^{34}\nu$	$1000(1-^{34}\nu/^{32}\nu)$
ν_1	345.43	343.41	5.85	345.43	344.75	1.97
ν_2	354.33	352.35	5.59	354.33	353.49	2.37
ν_3	479.38	470.18	19.19	479.38	479.14	0.50
ν_4	565.55	565.34	0.37	565.55	562.15	6.01
ν_5	577.94	577.71	0.40	577.94	574.65	5.69
ν_6	716.05	714.75	1.82	716.05	704.22	16.52
ν_7	1093.77	1093.76	0.01	1093.77	1089.40	4.00
ν_8	1249.02	1249.02	0.00	1249.02	1233.32	12.57
ν_9	1250.20	1250.19	0.01	1250.20	1234.47	12.58

Table 1. Calculated vibrational frequencies ($^{32}\nu$, $^{34}\nu$; cm^{-1}) and frequency shifts ($1000(1-^{34}\nu/^{32}\nu)$) of various sulfur species using the HF method

T(K)	HS^-	H_2S	SO_4^{2-}	Sulfane (SSO_3^{2-})	Sulfonate (SSO_3^{2-})
50	31.36	79.50	726.01	158.95	658.65
100	15.22	38.38	333.04	63.60	298.34
150	9.84	24.67	202.44	33.92	179.24
200	7.15	17.82	137.94	20.79	121.00
250	5.53	13.71	100.17	13.94	87.26
300	4.46	10.98	75.88	9.95	65.77
350	3.69	9.04	59.29	7.44	51.21
400	3.11	7.59	47.48	5.76	40.90
450	2.67	6.48	38.79	4.59	33.36
500	2.31	5.60	32.23	3.74	27.68
600	1.78	4.30	23.19	2.62	19.88
700	1.41	3.40	17.43	1.93	14.92
800	1.15	2.75	13.55	1.48	11.59
900	0.95	2.27	10.82	1.18	9.25
1000	0.79	1.90	8.84	0.95	7.55
1200	0.58	1.38	6.20	0.66	5.30

Table 2. Calculated reduced partition function ratios, 10^3 x $\ln(\beta_{34-32})$, of various sulfur species from 50 to 1200 K using the HF method

Figure captions

Figure 1. Disproportionation of thiosulfate by thiosulfate disproportionation bacteria in the enrichment culture obtained from tidal flat sediments at Weddewarden (Germany). Figure 1A shows the change in concentration measurement over time, and Figure 1B shows stable isotope data (Habicht et al., 1998).

Figure 2. Variation with time of the isotopic composition of each sulfur species at 150^{o}C (Uyama et al., 1985). (Image removed due to copyright restrictions.)

Figure 3. Comparison between the experimentally measured values (solid symbols) and calculated curve based on the experimental data for thiosulfate and sulfide (Chu et al., 2004).

Figure 4. Effect of temperature on the reduced partition function ratios, 10^3 x ln(β_{34-32}), of various sulfur species (50−170 °C) using the HF method.

Figure 5. Equilibrium fractionation factors plotted against temperature for various sulfur species. Four solid curves are derived from the reduced partition function ratios in Table 2. The broken curves and symbols are the experimental date.

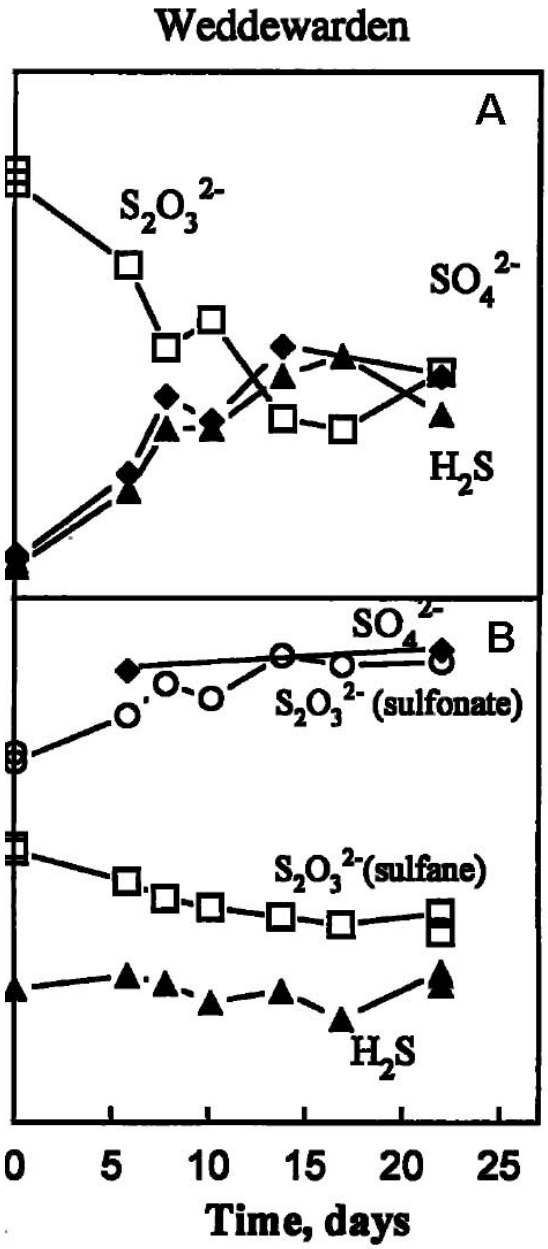

Figure 1

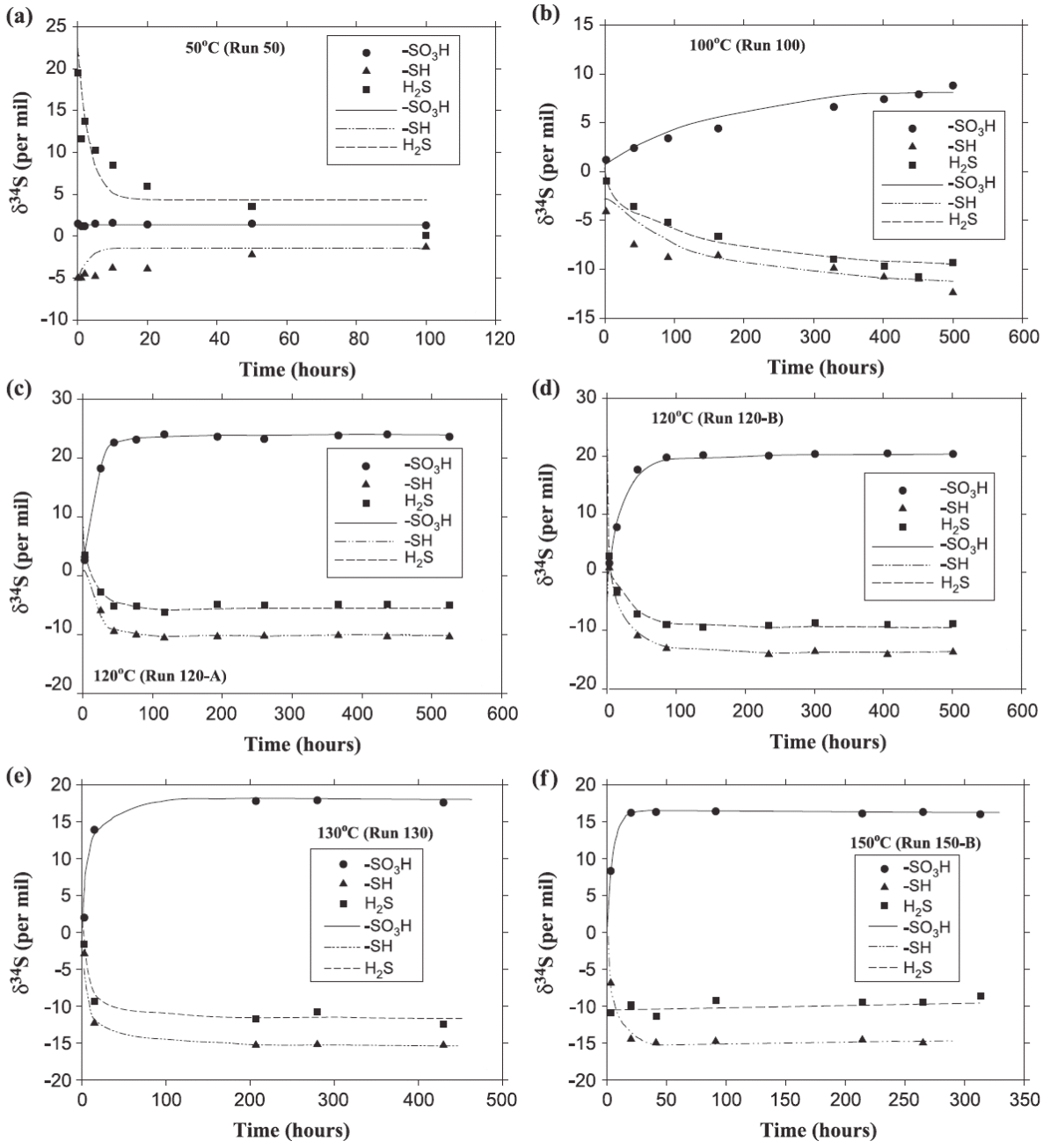

Figure 3

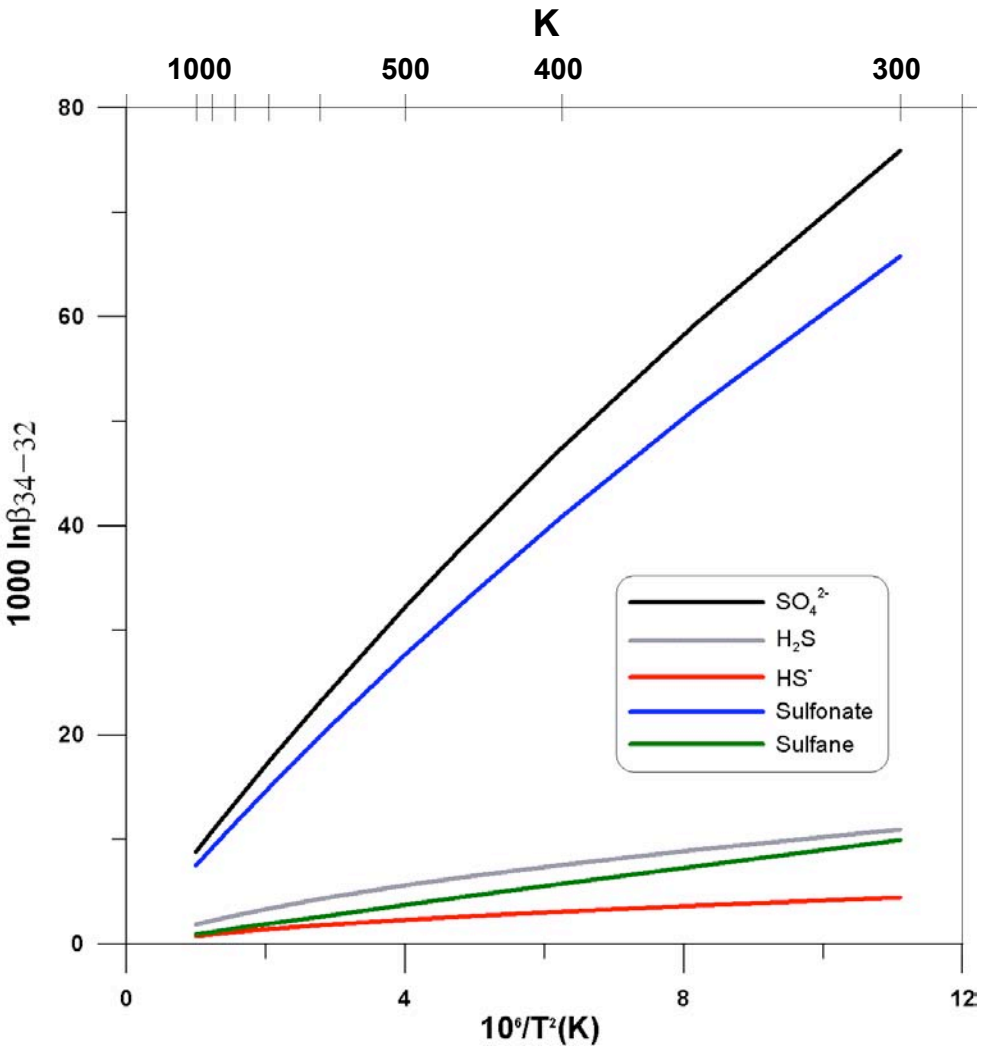
K
1000
500
400
300
80
60
40
20
0
1000 lnβ34−32
0
4
8
12
10⁶/T²(K)
SO4 2-
H2S
HS-
Sulfonate
Sulfane

Figure 4

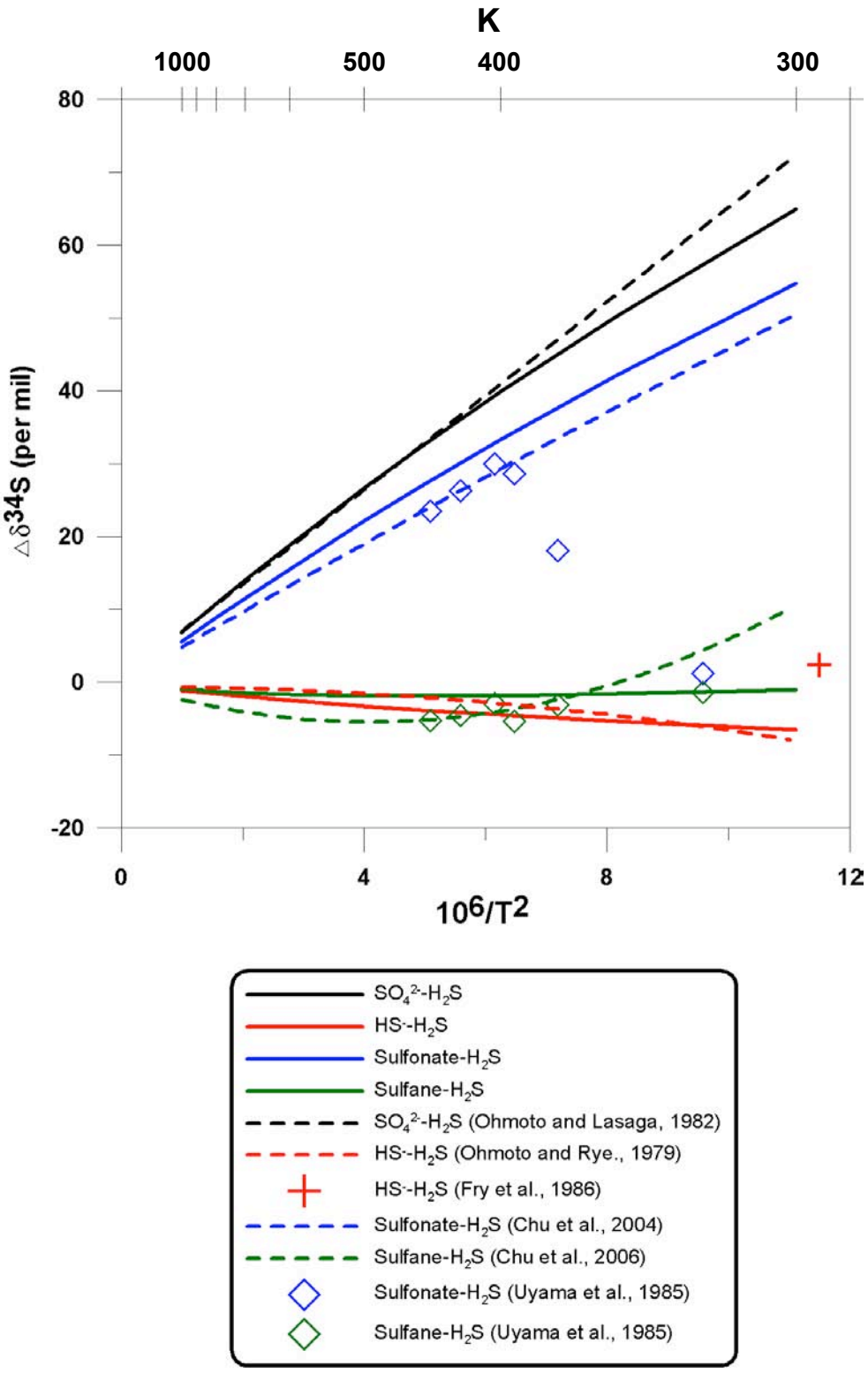
K
1000
500
400
300
80
60
40
20
0
-20
0
4
8
12
$\triangle\delta^{34}S$ (per mil)
$10^6/T^2$
SO_4^{2-}-H_2S
HS^--H_2S
Sulfonate-H_2S
Sulfane-H_2S
SO_4^{2-}-H_2S (Ohmoto and Lasaga, 1982)
HS^--H_2S (Ohmoto and Rye., 1979)
HS^--H_2S (Fry et al., 1986)
Sulfonate-H_2S (Chu et al., 2004)
Sulfane-H_2S (Chu et al., 2006)
Sulfonate-H_2S (Uyama et al., 1985)
Sulfane-H_2S (Uyama et al., 1985)

Figure 5